LA-UR -85-1135
CONF-850946--3

RECEIVED BY OSTI MAY 06 1985

MASTER

Los Alamos National Laboratory is operated by the University of California for the United States Department of Energy under contract W-7405-ENG-36

LA-UR--85-1135

DE85 010779

TITLE: THE MECHANICAL THRESHOLD OF DYNAMICALLY DEFORMED COPPER AND NITRONIC 40

AUTHOR(S): P. S. Follansbee, U. F. Kocks, and G. Regazzoni

SUBMITTED TO: International Conference on Mechanical and Physical Behavior of Materials under Dynamic Loading, Sept., 2-5, 1985, Paris, France

Los Alamos

Los Alamos National Laboratory
Los Alamos, New Mexico 87545

FORM NO 836 R4
ST NO 2629 5/81

THE MECHANICAL THRESHOLD OF DYNAMICALLY DEFORMED COPPER AND NITRONIC 40

P. S. Follansbee, U. F. Kocks, and G. Regazzoni

Los Alamos National Laboratory, Los Alamos, NM, USA

Résumé - On rapporte des mesures du seuil mécanique, ou contrainte seuil, effectuées sur des éprouvettes de cuivre et de Nitronic 40 déformées de manières quasi-statique et dynamique. Les résultats concernant le cuivre montrent que l'accroissement de la contrainte seuil avec la vitesse de deformation est semblable à celui de la contrainte d'ecoulement. Dans le case due Nitronic 40, les résultats donnent un rapport de la contrainte d'écoulement a la contrainte seuil de l'ordre de 0.6. Les deux résultats indiquent que la sensibilité croissante à la vitesse que l'on observe aux grandes vitesses de déformation pour ces matériaux n'est pas due à la prédominance d'un mécanisme de déformation de type frottement visqueux comme il a été parfois suggéré.

Abstract - Measurements of the mechanical threshold, or threshold stress, are reported on quasi-statically and dynamically deformed copper and Nitronic 40. The results for copper show that the increase of the threshold stress with strain rate is similar to that of the flow stress. In Nitronic 40 the results show that the ratio of the flow stress to the threshold stress is ~0.6. Both results indicate that the increased rate sensitivity found in these materials at high strain rates is not due to the predominance of a viscous drag deformation mechanism, as has been previously suggested.

1 - INTRODUCTION

It has long been known experimentally that a variety of metals show an increase in rate sensitivity when the imposed strain rate is raised above ~ 10^3 s^{-1}. Such an increase, for example, has been reported in annealed high purity iron by Davidson, Lindholm and Yeakley /1/, in aluminum by Hauser et al. /2/ and in copper by Kumar and Kumble /3/. There has been much discussion concerning the validity of these high strain rate experimental results (see, for example, Lindholm /4/). However, when split Hopkinson pressure bar (SHPB) techniques are used for the dynamic measurements, an extensive, numerical analysis of the SHPB test of Bertholf and Karnes /5/ has indicated that, if certain criteria regarding specimen dimensions, lubrication, and loading rate are satisfied, the results are valid at strain rates to roughly 10^4 s^{-1} /6/. Although evidence at higher strain rates than 10^4 s^{-1} is limited, measurements by Clifton, Gilat and Li on aluminum and copper /7/ and the analysis by Wallace /8/ of measurements by Johnson and Barker on 6061-T6 aluminum /9/ indicate higher flow stress levels in the shock regime than found at even those strain rates possible with SHPB techniques. Based on these results, it is concluded that the increased rate sensitivity in metals found under dynamic test conditions represents a real material response.

In the majority of the cases where the rate sensitivity has been found to increase, it has been suggested that the increased rate sensitivity is due to a transition in rate controlling deformation mechanism from thermal activation control of dislocation motion at low strain rates to viscous drag control at high strain rates. As evidence for this transition, some investigators have noted that the experimentally observed linear dependence of flow stress (at a uniform strain) on strain rate at high strain rates is consistent with the dislocation drag mechanism

/10/. Other investigators /11/ have emphasized that dislocation drag controlled deformation would indeed lead to a linear dependence of flow stress on strain rate, but the line would be required to pass through (or close to) the origin rather than through a large stress at zero strain rate, as is found experimentally. It has been suggested /12/ that an increasing mobile dislocation density (with stress) could provide the link between the experimental observations and the predicted behavior based on dislocation drag controlled deformation.

Whether or not the high strain rate test results described above extrapolate to the origin is one criteria that, if satisfied, would support the proposed transition in rate controlling deformation mechanism. However, as indicated above, the experimental results can be made to fit such a theory by imposing a minor and not unrealistic condition regarding the mobile dislocation density. Another more restrictive condition is that when dislocation drag effects dominate the deformation kinematics, the applied stress must be on the order of or greater than the strength of the dominant barrier that restricts deformation at lower strain rates or higher temperatures /13/. In Follansbee, Regazzoni and Kocks /13/, the mechanical threshold (flow stress at 0 K), which provides an indication of the barrier strength, was measured on dynamically deformed OFE copper. The mechanical threshold was found to exceed the flow stress. A model of the deformation kinematics, which included a stress dependent mobile dislocation density, was used to fit the experimental results over a wide range of strain rates. The model assumed that the measured mechanical threshold varied with strain, but not with strain rate, i.e., strain was assumed to be a state parameter. There were several features of the experimental results which were inconsistent with this assumption and which were noted in /13/.

The purpose of this work is to show how the mechanical threshold varies with strain and strain rate over a wide range of conditions. These findings enable an evaluation of the constant structure assumption made in /13/ (and by others) and to a further evaluation of the dislocation drag deformation mechanism which is postulated to explain the increased rate sensitivity found at high strain rates.

In section 2, the experimental procedure for determining the mechanical threshold is reviewed. In particular, it is shown how the temperature dependence of the shear modulus must be included in the data analysis procedure; this was neglected in /13/. In section 3, the measured mechanical threshold values are reported for a wide range of strain rates and strains for OFE copper and for a wide range of strain rates, but only a single strain, for Nitronic 40 stainless steel. The mechanical threshold values are then compared with the accompanying flow stress values. In section 4, the implications of the results concerning the rate controlling deformation mechanism are discussed.

2 - MEASUREMENT OF THE MECHANICAL THRESHOLD

Copper was chosen for this investigation since it is a simple, single phase FCC metal with well documented quasi-static deformation mechanisms. Oxygen-free electronic (OFE) copper (ASTM C10100) in the form of 0.95 cm diameter rods were procurred in the as-wrought form. Compression specimens were machined according to the dimensions described below. Following machining the specimens were annealed at 600 C for one hour in vacuum which yielded an approximately equiaxed structure with an average grain diameter of ~40 μm.

A less extensive set of measurements was performed with Nitronic 40, which is a manganese bearing austenitic stainless steel often referred to as 21-6-9. It had the following composition: 20% (by weight) Cr; 6.6% Ni; 8.8% Mn; 0.18% P; 0.18% S; 0.01% C; and 0.32% N. The Nitronic 40 was also studied in the annealed condition with an average grain diameter of ~40 μm.

The procedure for measuring the mechanical threshold has been previously outlined /13/. Multiple specimens (usually 8) are prestrained at room temperature along the strain rate and strain path of interest and then unloaded. This prestrain produces

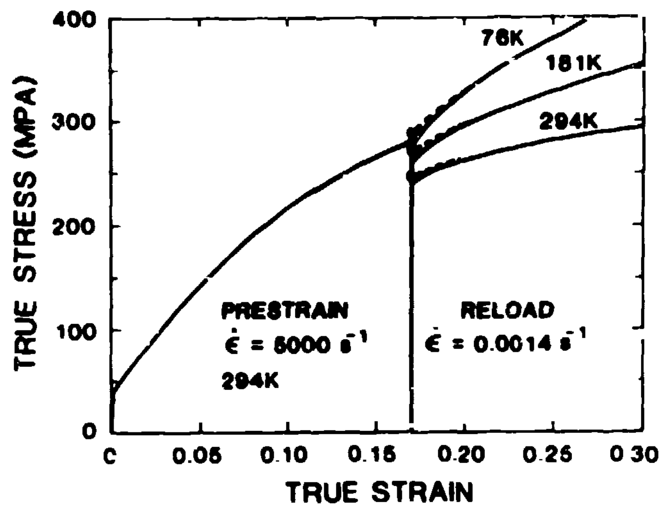

Fig. 1 - Stress strain curves for the dynamic prestrain and quasi-static reload of copper to measure the mechanical threshold (threshold stress).

a structure which is characteristic of the strain and strain rate path; we now want to probe this structure. To determine the flow stress at 0 K, the specimens are reloaded at a conveniently low strain rate (0.0014 s^{-1}) and at temperatures of 76 K, ~180 K, and 295 K and the yield stress is recorded. For the copper experiments, nominal true strain rates of 10^{-4} s^{-1}, 10^{-2} s^{-1}, 10^{0} s^{-1}, 10^{2} s^{-1}, 2×10^{3} s^{-1}. 5×10^{3} s^{-1}, and 10^{4} s^{-1} and true strains of 0.05, 0.10, 0.15, 0.20 and 0.25 were chosen for investigation; this yielded 35 separate strain and strain rate histories. Specimen dimensions were chosen such that after the prescribed prestrain, the diameter and length of each specimen equaled 0.508 cm. For the stainless steel experiments, only the following two histories were investigated: strain rates of 10^{-3} s^{-1} and 6×10^{3} s^{-1} to a strain of 0.10.

Three mechanical test machines were utilized for these compression tests. For experiments at strain rates less than 10^{-1} s^{-1}, which includes all of the reloading experiments, a standard screw-driven mechanical testing machine was used. Reload experiments at room temperature, 76 K (with liquid nitrogen), and 180 K to 200 K (with freezing methanol) were performed with a completely immersible subpress. Powdered boron nitride was chosen as the lubricant for these low temperature experiments, whereas molybdenum disulfide was used for all room temperature testing. A servo-hydraulic testing machine was used for strain rates to 10^{2} s^{-1} and a SHPB was used for testing at strain rates to 10^{4} s^{-1} /6/. To facilitate loading to a constant strain in the SHPB, a 0.508 cm deep by 0.64 cm diameter flat-bottomed hole was drilled into the end of the 1.1 cm diameter transmitter bar.

An example of the prestrain and reloading stress strain curves for copper prestrained at 5000 s^{-1} to a nominal true strain of 0.15 and reloaded at a strain rate of 0.0014 s^{-1} is shown in Fig. 1. Although the specimens were stored in liquid N_2 immediately after the prestrain and until reloading, the reload traces in Fig. 1 show an indication of recovery in the immediate yield region. The actual details in this region were far less reproducible than was the large strain work hardening behavior. Thus the flow stress upon reloading was determined by back extrapolating the work hardening behavior to the elastic line, as is shown with the dashed lines in Fig. 1.

Another difficulty encountered in the SHPB experiments was that axial inertia led to continued deformation after the specimen/incident bar interface was unloaded (i.e., after the specimen length decreased below 0.508 cm) [1]. This extra deformation was

[1] This problem was only significant in the copper experiments, which is consistent with the fact that the velocity of the plastic unloading wave varies with stress /14/, which in the stainless steel was ~4 times that in the copper.

nonuniform, being minimum at the specimen/incident bar interface and maximum at the specimen/transmitter bar interface, and became more severe as the strain rate increased. Two problems were introduced by this nonuniform deformation. First of all, the slightly bell-shaped samples would have complicated the interpretation of the subsequent reloading step; this problem was circumvented by remachining each specimen to a cylindrical geometry (which added an additional ~ 30 minutes to the time spent at room temperature). The second problem was in relating the measured mechanical threshold to a "strain". Since upon reloading, the yield stress would represent the section of the specimen which had received the smallest post-uniform deformation, the strain was computed at the smallest diameter of the deformed specimen, which was generally at or near the incident bar/specimen interface. For the case shown in Fig. 1, the strain measured was 0.168 rather than the desired 0.15. The mechanical threshold at the strain of interest was then estimated by interpolating between actual measured strains.

2.1 <u>EXTRAPOLATION TO 0 K</u>. The results shown in Fig. 1 give the variation of the flow stress with reloading temperature to a minimum temperature of 76 K. An extrapolation is required to estimate the flow stress at 0 K. The manner in which the flow stress varies with temperature depends on the details of the rate controlling deformation mechanism. In pure copper at low strain rates, deformation is controlled by the interaction of mobile dislocations with forest dislocations which is a thermally activated process. The relationship between applied stress, strain rate, and temperature at constant structure is best described by a law of the form /15/

$$\dot{\varepsilon} = \dot{\varepsilon}_o \exp\left[\frac{-\Delta G}{kT}\right] , \qquad (1)$$

where the stress dependence enters through the activation free enthalpy ΔG when written as

$$\Delta G = F_o\left[1 - (\sigma/\hat{\tau})^{1/2}\right]^{3/2} . \qquad (2)$$

In the above expressions, $\dot{\varepsilon}_o$ is a constant of the order of 10^8 s^{-1}, k is Boltzman's constant, T is the temperature and F_o is the Helmholz free energy. The mechanical threshold $\hat{\tau}$ in Eq. 2 is written here as a normal (rather than shear) stress; it is called $\hat{\tau}$ instead of σ to emphasize that it is a material property. In addition to the explicit temperature dependence described in Eq. 1, it is important to also include the temperature dependence of the activation free enthalpy (which is assumed to be that of the shear modulus μ /15/) by rewriting Eq. 2 as

$$\Delta G = \mu(t)b^3\, g\left(\frac{\sigma}{\mu}\right) = \mu(T)b^3\, g\left[1 - \left(\frac{\sigma/\mu(T)}{\hat{\tau}/\mu(T)}\right)^{1/2}\right]^{3/2} , \qquad (3)$$

where g is the normalized activation free enthalpy. Combining Eq. 3 with Eq. 1 and rearranging gives

$$\left(\frac{\sigma}{\mu(T)}\right)^{1/2} = \left(\frac{\hat{\tau}}{\mu(T)}\right)^{1/2} \left[1 - \left(\ln\frac{\dot{\varepsilon}_o}{\dot{\varepsilon}} \frac{kT}{\mu(T)b^3 g}\right)^{2/3}\right] . \qquad (4)$$

If the normalization with respect to temperature is correct, then a plot of $[\sigma/\mu(T)]^{1/2}$ versus $[kT/\mu(T)b^3]^{2/3}$ for the reload experiments at constant strain rate but varying temperature should yield a straight line. The intercept at zero temperature in this plot gives the mechanical threshold normalized by the shear modulus while the slope is inversely related to the normalized activation free enthalpy.

Values for the shear modulus are given in Table 1. For copper these values represent the single crystal shear modulus /16/. The elastic constants required to calculate the single crystal shear modulus are unavailable for the particular stainless steel used in this investigation. In addition, we could find no reported data for the polycrystal shear modulus at low temperature. Thus, the data in Table 1 for Nitronic 40 represent an extrapolation to low temperatures of data measured on a similar material at ambient and elevated temperature /17/. The slope $d\mu/dT$

reported in /17/ ($d\mu/dT$ = -.032 GPa/K) is identical to that measured at low temperature on a variety of austenitic stainless steels (Armstrong, to be published). In making this extrapolation we are assuming that the low temperature elastic modulus anomaly, which is often found in austenitic stainless steels (Armstrong, to be published), occurs in Nitronic 40 at a temperature below 76 K.

TABLE 1 Temperature Dependence of the Shear Modulus

T (K)	μ (GPa) Copper	μ (GPa) Nitronic 40
76	45.45	84.3
180	44.07	81.0
295	42.17	77.3

3. RESULTS

3.1 MECHANICAL THRESHOLD IN COPPER. An example of the variation of the normalized reload stress versus normalized test temperature for copper is shown in Fig. 2. Results in this figure are for a prestrain path at a strain rate of 0.00014 s^{-1} to the strain indicated. For each prestrain at least two specimens were tested at each reload temperature. (Only one data point is shown when two tests gave the same result.) A straight line is seen to fit each set of data as shown; this tends to support the thermal activation law given by Eqs. 1 and 2 and the normalization procedure described by Eq. 3. As expected the mechanical threshold increases with strain, and the rate of this increase decreases with strain. An unexpected result is that the slope of the line increases slightly with strain which indicates that the normalized activation free enthalpy decreases as the mechanical threshold (strain) is increased. This, however, is only a small effect.

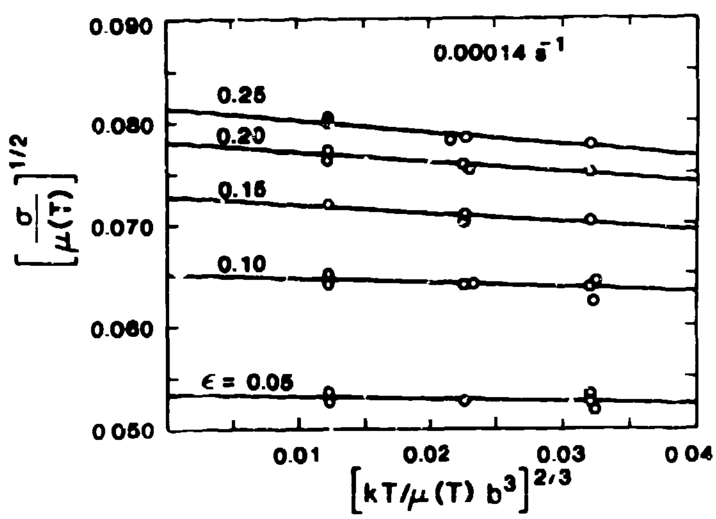

Fig. 2 - Normalized data for the reload yield stress versus test temperature for the prestrain of copper at a strain rate of 0.00014 s^{-1} to the strain noted.

Figure 3 shows the results at uniform strain but varying strain rate. Here, the important observation is that at uniform strain the mechanical threshold is an increasing function of strain rate. Once again, the slope of the fit in Fig. 3 increases slightly with increasing mechanical threshold (strain rate).

All of the results for copper, including the mechanical threshold and flow stress values, are tabulated in Tables 2 and 3. The values for the mechanical threshold listed in these tables are referenced to 295 K since this is the temperature at which the prestrains were introduced. The mechanical threshold at 295 K represents the strength of the average barrier encountered by mobile or potentially mobile dislocations during the prestrain. A comparison of the threshold stress with the flow stress listed in the last column of Tables 2 and 3 indicates that in each case

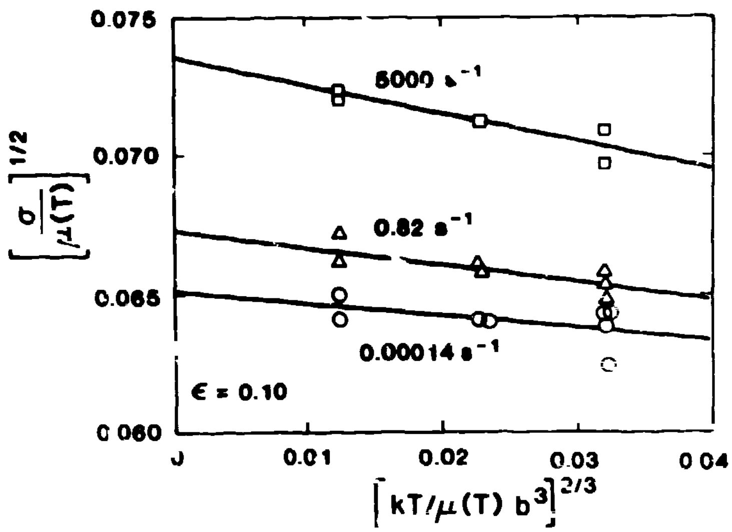

Fig. 3 - Normalized data for the reload yield stress versus test temperature for the prestrain of copper at the strain rate noted to a strain of 0.10.

the former stress exceeds the latter. Also included in these tables is the standard error for the estimate of $\hat{\tau}$. In a few cases, this error was quite large; this was particularly true at low strains where the slope of the fit approached zero.

TABLE 2 Mechanical Threshold Values for Copper at $\dot{\varepsilon} < 100\ s^{-1}$

$\dot{\varepsilon}$, s^{-1}	ε	$\hat{\tau}$, MPa	s.e.*, MPa	σ, MPa
0.00014	0.05	120	18	114
	0.10	179	17	168
	0.15	223	10	206
	0.20	257	4	234
	0.25	279	3	252
0.015	0.05	125	28	118
	0.10	187	15	175
	0.15	235	3	218
	0.20	269	6	247
	0.25	294	4	269
0.82	0.05	134	70	127
	0.10	191	5	180
	0.15	244	6	224
	0.20	284	3	268
	0.25	309	3	295
81	0.05	134	35	130
	0.10	207	5	194
	0.15	251	4	241
	0.20	299	2	281
	0.25	329	2	307

* Standard error on estimate of $\hat{\tau}$

The dynamic test results for copper are listed in Table 3. The mechanical threshold values listed in the third column correspond to the actual values at the strain indicated. The values listed in the sixth column are interpolated (or extrapolated) values which enable a constant strain comparison with the values listed in Table 2. Although the standard error for the estimate of $\hat{\tau}$ is uniformly low for the results listed in Table 3, the error in the estimate of the corresponding strain, due to the nonuniform deformation described earlier, is likely much larger.

TABLE 3 Mechanical Threshold Values for Dynamically Deformed Copper

$\dot{\varepsilon}$, s^{-1}	ε	$\hat{\tau}$, MPa	s.e., MPa	ε	$\hat{\tau}$, MPa	σ, MPa
1800	0.064	172	25	0.05	141	121
	0.107	218	2	0.10	217	195
	0.152	280	3	0.15	273	250
	0.209	309	3	0.20	313	297
	0.253	347	2	0.25	342	318
5000	0.065	178	6	0.05	145	132
	0.10	228	7	0.10	224	206
	0.168	285	2	0.15	281	260
	0.211	325	1	0.20	321	305
	0.257	359	2	0.25	351	329
9500	0.087	212	5	0.05	152	146
	0.134	272	2	0.10	234	220
	0.156	300	4	0.15	291	274
	0.189	329	2	0.20	331	317
	0.226	343	1	0.25	359	343

The flow stress and mechanical threshold results at strains of 0.10 and 0.20 are plotted together in Figs. 4 and 5. Figure 4 is a semi-logarithmic representation which includes data at all strain rates. As indicated in the Introduction, the strain rate dependence of the flow stress begins to increase fairly dramatically when the strain rate is raised above ~10^3 s^{-1}. The interesting observation in Fig. 4 is that the mechanical threshold increases along with the flow stress. The dynamic test results are plotted on linear axes in Fig. 5. Here it is evident that the increase in the mechanical threshold with increasing strain rate is approximately parallel to the increase in flow stress.

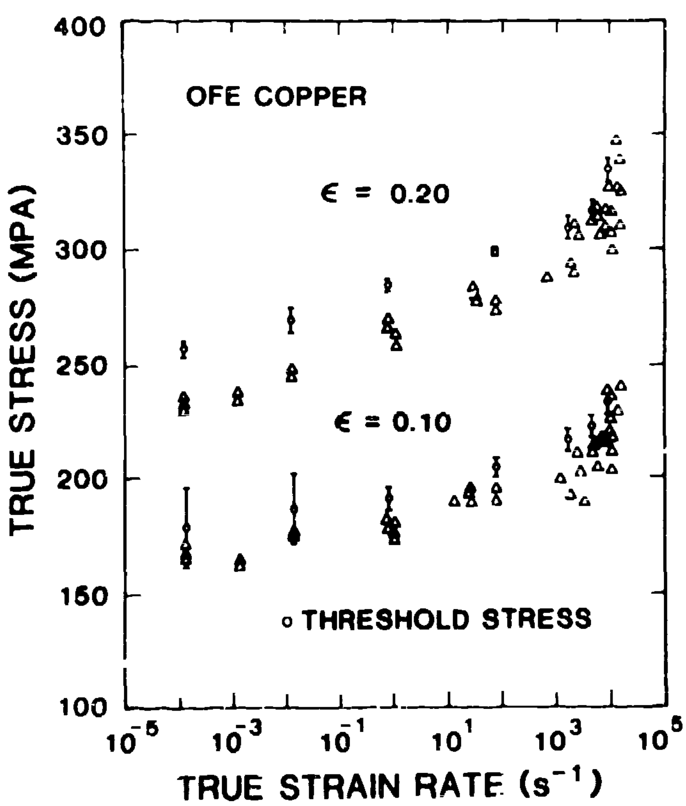

Fig. 4 - Strain rate dependence of the flow stress (triangles) and threshold stress (circles) of copper at strains of 0.10 and 0.20.

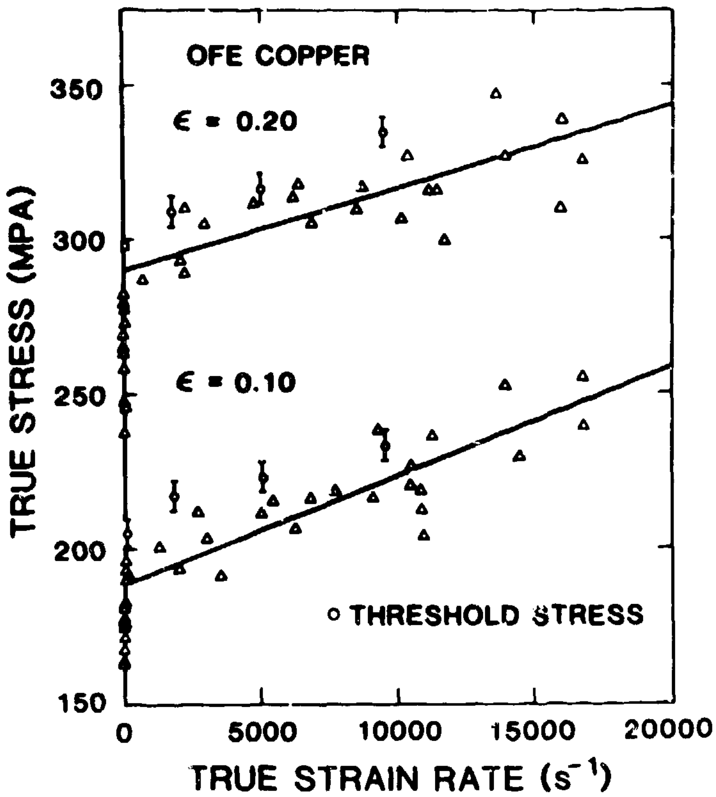

Fig. 5 - Strain rate dependence of the flow stress (triangles) and threshold stress (circles) of copper at strains of 0.10 and 0.20.

3.2 MECHANICAL THRESHOLD IN NITRONIC 40. A plot of the normalized stress versus normalized temperature for the two strain rates investigated is shown in Fig. 6. The most prominent difference between the data for copper shown in Fig. 3 and that for Nitronic 40 shown in Fig. 6 is in the slope of the line, which is much higher in the latter case. This indicates that the dominant obstacle to dislocation motion in Nitronic 40 has a lower free enthalpy and thus is much more strain rate (and temperature) sensitive. The mechanical threshold and flow stress values for Nitronic 40 are tabulated in Table 4. Note that for this material the ratio of the flow stress to the mechanical threshold is much smaller than it was for copper.

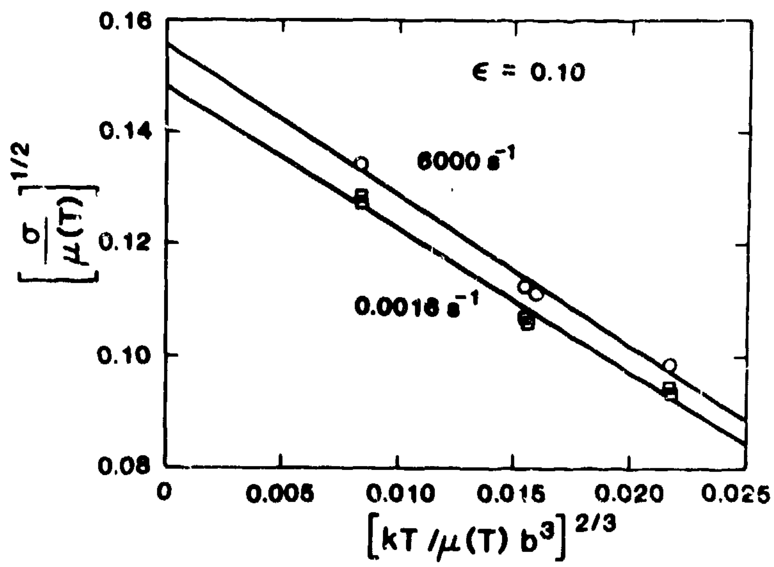

Fig. 6 - Normalized data for the reload yield stress versus test temperature for the prestrain of Nitronic 40 at strain rates of 0.0016 and 6000 s^{-1} to a strain of 0.10.

TABLE 4 Mechanical Threshold Values for Nitronic 40

$\dot{\varepsilon}$, s^{-1}	ε	$\hat{\tau}$, MPa	s.e., MPa	σ, MPa
0.0016	0.10	1696	42	689
6000	0.10	1874	31	1125

The flow stress and mechanical threshold values are plotted together on semi-logarithmic axes in Fig. 7. Once again the increased rate sensitivity of the flow stress is found at high strain rates [2]. For Nitronic 40, however, this increase in flow stress is not accompanied by as significant an increase in the mechanical threshold as was found in copper.

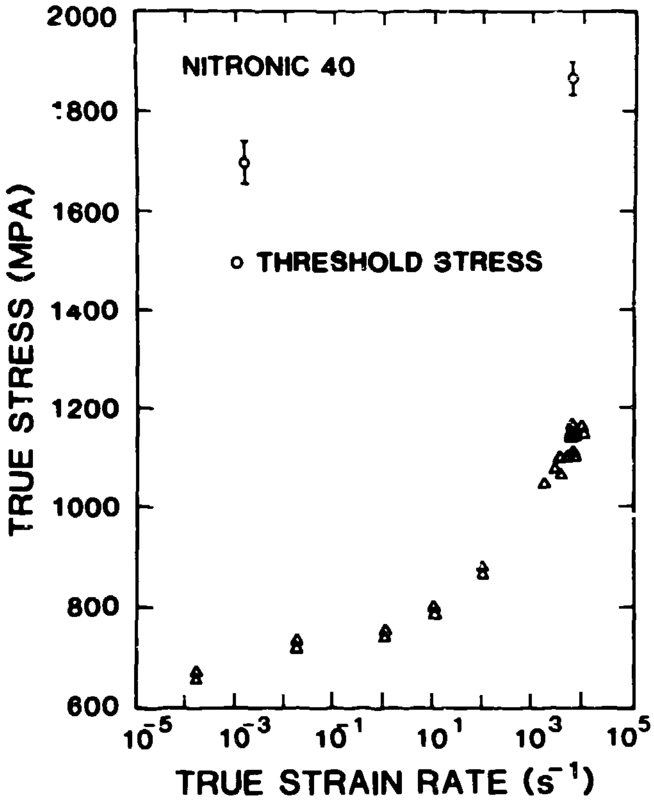

Fig. 7 - Strain rate dependence of the flow stress (triangles) and threshold stress (circles) in Nitronic 40 at a strain of 0.10.

4. DISCUSSION

Two significant findings have evolved from these mechanical threshold measurements. The first is that for copper the increased rate sensitivity found on a constant strain comparison of flow stress data is accompanied by an identical increase in the mechanical threshold. Although not illustrated here, it is evident from inspection of he data in Tables 2 and 3 that a comparison at constant structure would show no dramatic increase in rate sensitivity. For example, the flow stress at a strain rate of 0.015 s^{-1} to a strain of 0.15 ($\hat{\tau}$ = 235 MPa) is only slightly less than the flow stress at a strain rate of 9500 s^{-1} to a strain of 0.10 ($\hat{\tau}$ = 234 MPa). Thus the "increased rate sensitivity" in copper is simply (or not so simply) due to structure evolution. The details of the evolutionary process are not the subject of this paper. However, the mechanical threshold measurements do lead us to conclude

[2] In fact, for this material, the increase appears to begin at strain rates as low as 10^2 s^{-1}. Since the experimental techniques and data interpretation are without question at such low strain rates, this is strong evidence that the increased rate sensitivity found with the SHPB is a real effect.

that efforts to understand the increased rate sensitivity should concentrate on the rate sensitivity of structure evolution rather than on the contribution of another deformation mechanism such as viscous drag.

The data for Nitronic 40 provide the second significant result. In this material, an increased rate sensitivity at high strain rates is noted, yet the ratio of the flow stress to the mechanical threshold is only ~0.6. Since the mechanical threshold is changing less rapidly in comparison to the flow stress than was found in copper, the Nitronic 40 results more closely approximate the constant structure conditions modelled in /13/. One conclusion from that model was that for dislocation drag to be important, the flow stress must be approximately equal to or greater than the mechanical threshold. This is not the case for Nitronic 40; thus, we conclude that in this material as well as in copper, the observed increased rate sensitivity is not due to a transition in rate controlling deformation mechanism.

We do not imply by these conclusions that viscous drag is not an important deformation mechanism; under the right structure and applied stress conditions, deformation will become limited by visous forces on dislocations. However, these processes do not appear to be important for deformation in copper and Nitronic 40 at strain rates up to 10^4 s^{-1}.

ACKNOWLEDGMENTS

We are grateful for the assistance of W. J. Wright in performing the SHPB tests and of M. L. Lopez in performing the low and medium rate experiments. This work was performed under the auspices of the U. S. Department of Energy.

REFERENCES

/1/ Davidson, D. L., Lindholm, U. S. and Yeakley, L. M., Acta Met. 14 (1966) 703.
/2/ Hauser, F. E., Simmons, J. A. and Dorn, J. E., in Response of metals to high velocity deformation, ed. P.G. Shewmon and V. F. Zackary (New York, Interscience) (1961) 93.
/3/ Kumar, A. and Kumble, R. G., J. Appl. Phys. 40 (1969) 3475.
/4/ Lindholm, U. S., in High rate deformation of solids, ed. K. Kawata and J. Shioiri (New York, Springer-Verlag) (1978) 26.
/5/ Bertholf, L. D. and Karnes, C. H., J. Mech. Phys. Solids 23 (1975) 1.
/6/ Frantz, C. E., Follansbee, P. S. and Wright, W. J., in High energy rate fabrication, ed. I. Berman and J. W. Schroeder (New York, Am. Soc. Mech. Engr.) (1984) 229.
/7/ Clifton, R. J., Gilat, A. and Li, C. H., in Material behavior under high stress and ultrahigh loading rates, ed. J. Mescall and V. Weiss (New York, Plenum) (1983) 1.
/8/ Wallace, D. C., Phys. Rev. B22 (1980) 1487.
/9/ Johnson, J. N. and Barker, L. M., J. Appl. Phys. 40 (1969) 4321.
/10/ Kumar, A., Hauser, F. E. and Dorn, J. E., Acta Met. 16 (1968) 1189.
/11/ Klahn, D., Mukherjee, A. K. and Dorn, J. E., in Strength of metals and alloys (Am. Soc. Metals) (1970) 951.
/12/ Frost, H. J. and Ashby, M. F., J. Appl. Phys. 42 (1971) 5273.
/13/ Follansbee, P. S., Regazzoni, G. and Kocks, U. F., in Mechanical properties at high rates of strain, ed. J. Harding (Inst. of Phys.) (1984) 71.
/14/ Mott, N. F., Proc. Roy. Soc. London 189A (1947) 300.
/15/ Kocks, U. F., Argon, A. S. and Ashby, M. F., Thermodynamics and kinetics of slip, Prog. Mat. Sci. 19 (New York, Pergamon) (1975).
/16/ Overton, W. C. and Gaffney, J., Phys. Rev. 98 (1955) 969.
/17/ Garofalo, F., Proc. Am. Soc. Test. Mat. 60 (1960) 738.